Bioorganic Chemistry 181 (2026) 110323

Contents lists available at ScienceDirect

Bioorganic Chemistry

journal homepage: www.elsevier.com/locate/bioorg

An affordable and low-waste protocol for rapid and robust solid-phase peptide synthesis at elevated temperatures

Giacomo Bettin [a,b,1], Matilde Salvadoretti [c,2], Guglielmo Rossi [c], Fabrizio Fabris [c,3], Alessandro Bonetto [d,4], Claudio Brancolini [a,5], Alessandro Scarso [c,*,6], Alessandro Angelini [b,c,e,7,*]

[a] Department of Medicine, Università degli Studi di Udine, p.le Kolbe 4, 33100, Udine, Italy
[b] Arzanya S.r.l., Via Rezzonico 6, 35131, Padova, Italy
[c] Dipartimento di Scienze Molecolari e Nanosistemi, Università Ca' Foscari Venezia, via Torino 155, Mestre, Venezia, 30172, Italy
[d] Dipartimento di Scienze Ambientali Informatica e Statistica, Università Ca' Foscari Venezia, via Torino 155, Mestre, Venezia, 30172, Italy
[e] European Centre for Living Technology (ECLT), Ca' Bottacin, Dorsoduro 3911, Calle Crosera, 30123 Venezia, Italy

ARTICLE INFO

Keywords:
Solid-phase peptide synthesis
High-temperature peptide coupling
Peptide epimerization
Rapid synthesis
Waste minimization

ABSTRACT

Automated solid-phase peptide synthesis (SPPS) is the premier methodology for producing high-purity peptides across a broad range of applications. However, despite its efficiency, automated SPPS often requires expensive instrumentation and generates significant chemical waste. To overcome these limitations, we present a robust SPPS protocol that competes the thermal acceleration of microwave-assisted systems using standard laboratory equipment, offering a highly accessible and cost-effective alternative. The methodology enables the rapid assembly of a diverse array of linear and cyclic peptides (10–100 mg scale), including two biochemical active sequences, with reaction times reduced to minutes and a decrease in chemical waste. Given that elevated temperatures could compromise stereochemical integrity, we performed an in-depth investigation into epimerization risks using a multi-modal analytical suite, including high-performance liquid chromatography, nuclear magnetic resonance, and ion mobility mass spectrometry. Our results demonstrate that this instrumental approach not only provides satisfactory crude yields and purities but also maintains high stereochemical fidelity and native biochemical function, offering a robust alternative to high-cost automated systems.

1. Introduction

Solid-phase peptide synthesis (SPPS) is widely regarded as a mature cornerstone of organic synthesis. Automated platforms operating on resin are now ubiquitous, routinely delivering high-purity peptides in 10–20 amino acid sequences on typical 5–100 μmol scales. Despite this maturity, the demand for rapid, reliable, and sustainable peptide assembly continues to surge, driven by expanding applications in medicinal chemistry [1]—ranging from oncology to infectious diseases—as well as in hydrogel materials [2], organocatalysis [3], and other emerging peptide technologies [4]. Over the years different methodological approaches have been proposed to accelerate peptide synthesis and to minimize its environmental impact due to high waste production [5] related to the large use of polar aprotic solvents like dimethylformamide (DMF), dimethyl sulfoxide (DMSO) or chlorinated dichloromethane (DCM) and reagents excesses. Major steps toward more efficient and sustainable SPPS [6] are based on the use of microwave reactors (MW) [7], ball milling [8] in particular to reduce solvent

* Corresponding authors at: Dipartimento di Scienze Molecolari e Nanosistemi, Università Ca' Foscari Venezia, via Torino 155, Mestre, Venezia, 30172, Italy.
E-mail addresses: alesca@unive.it (A. Scarso), alessandro.angelini@unive.it (A. Angelini).
[1] ORCID ID: https://orcid.org/0009-0003-3511-6679
[2] ORCID ID: https://orcid.org/0009-0005-4234-384X
[3] ORCID ID: https://orcid.org/0000-0001-9209-1680
[4] ORCID ID: https://orcid.org/0000-0002-1642-2553
[5] ORCID ID: https://orcid.org/0000-0002-6597-5373
[6] ORCID ID: https://orcid.org/0000-0001-6114-9181
[7] ORCID ID: https://orcid.org/0000-0001-5923-3843

https://doi.org/10.1016/j.bioorg.2026.110323
Received 7 June 2026; Received in revised form 9 July 2026; Accepted 1 August 2026
Available online 7 August 2026

use [9] and flow-based peptide synthesis [10].

However, the requirement for costly, specialized instrumentation often precludes widespread adoption by research groups lacking dedicated infrastructure. Consequently, a shift toward 'democratizing' accelerated SPPS through affordable, accessible apparatuses has emerged to perform peptide synthesis efficiently and on scale of 10–100 mg. Recent contribution by Hurevich and collaborators described a heated vortex reactor underlying the importance of proper stirring and high temperature reaction conditions, demonstrating the robustness of the method on notoriously difficult to synthesize peptides [11]. During the preparation of this contribution, Benoit and collaborators described a simple system based on syringes for SPPS immersed in a 75 °C water bath [12]. Both methods enabled purity profiles comparable to MW or mechanochemical methods.

Building upon this paradigm, we herein report an efficient and accessible protocol for high-temperature SPPS on a 10–100 mg, offering a practical alternative to more expensive MW systems. Our approach utilizes a standard laboratory magnetic stirrer equipped with an aluminium heating block to manifold syringes, enabling rapid peptide couplings at 90 °C under magnetic stirring. This setup allows for the synthesis of both linear and cyclic peptides on various solid supports with good purity profiles, reducing reaction times to minutes while curtailing chemical waste. Crucially, the application of high thermal energy in peptide coupling raises valid concerns regarding stereochemical integrity—an aspect frequently under-investigated in rapid SPPS method development [13]. To rigorously validate our methodology against literature standards, we performed an in-depth analysis of epimerization risks. We employed a comprehensive analytical approach combining high-performance liquid chromatography (HPLC), 1D and 2D nuclear magnetic resonance (NMR), and ion mobility mass spectrometry (IM-MS) to probe for partial epimerization. Furthermore, analysis of two different biochemical active peptides synthesized by both our high-temperature protocol and standard room-temperature methods revealed comparable binding affinities and inhibitory potencies. Our results demonstrate that this approach not only provides satisfactory crude yields and purities but also maintains high stereochemical fidelity and native biochemical function, offering a robust alternative to high-cost automated systems.

2. Results and discussion

We developed a simple SPPS apparatus consisting of a custom aluminium block designed to accommodate standard reaction syringes. Mounted on a magnetic stirrer, this setup provides precise temperature control while ensuring efficient mixing via internal magnetic bars (**Supplementary fig. 1**). While racemization during carboxyl activation is a thoroughly characterized phenomenon in room-temperature peptide synthesis [13], driving the development of stereoselective activation methods, the extent of epimerization at elevated temperatures remains insufficiently studied. To investigate this, we synthesized a model dipeptide sequence (**1**) containing *L*-phenylglycine (Phg), a non-canonical amino acid chosen for its pronounced propensity for epimerization, thereby making its stereochemical retention highly dependent on specific experimental parameters [14] (Scheme 1). Toward this goal we applied the following protocol: *i*) Rink-Amide resin (100 mg) swelling (DMF 5 mL × 2 × 45 min at 25 °C), *ii*) Fmoc deprotection using piperidine 20% in DMF (0.1 M Oxyma Pure) 3 mL × 1 × 1 min, 90 °C, 300 rpm), *iii*) single coupling (Fmoc-amino acid 5 eq., Oxyma Pure 5 eq., DIC 5 eq., DMF 5 mL, 1 × 5 min, 90 °C, 300 rpm), *iv*) wash with DMF (3 mL × 3) after every step and *v*) cleavage cocktail using 7.5 mL 95% TFA, 2.5% TIS, 2.5% water, 2.5 h, 25 °C.

The optimization of reaction parameters, including coupling reagents, amino acid stoichiometry, temperature, and reaction time, is summarized in **Table 1**. To better assess the reaction performances, we compared the standard protocol based on diisopropylcarbodiimide (DIC)/ethyl cyano(hydroxyimino)acetate (Oxyma Pure) with that based on hexafluorophosphate benzotriazole tetramethyl uronium (HBTU). These parallel synthetic routes facilitated the validation of HPLC and NMR analytical methods for determining the stereochemical purity of the target dipeptides (**Supplementary figs. 2–13**). Notably, the use of HBTU (**Table 1**, entry 1) resulted in loss of stereochemical integrity, yielding a mixture of epimers consistent with the extensive racemization of the Phg residue (Fig. 1).

Significant epimerization was evident from the ^{1}H NMR analysis of the crude dipeptide. The spectrum displayed two overlapping doublets at δ 5.40 ppm, assigned to the α-proton of the Phg residue in the L-Arg-L-Phg and L-Arg-D-Phg diastereomers. Integration of the distinct Phg NH resonances at δ 8.50 and 8.63 ppm revealed a 50:50 diastereomeric ratio, a result corroborated by HPLC analysis (Fig. 1a). In contrast, the employment of the DIC/Oxyma Pure coupling system (Fig. 1b and **Table 1**, entry 2) resulted in the formation of a single species. The exclusive formation of the desired L-Arg-L-Phg stereoisomer was confirmed by both ^{1}H NMR and HPLC (Fig. 1). These data demonstrate the superior efficacy of DIC/Oxyma Pure [15–17], which enables high-temperature peptide coupling at short reaction times while maintaining the stereochemical integrity of the activated amino acid. Notably, the same stereochemical outcome was consistently observed across three independent synthetic batches of the model dipeptide Arg-Phg (**Table 1**, entries 3) (**Supplementary figs. 7**).

To further optimize the method, we adjusted the reaction parameters by decreasing the reaction time to 3 min, reducing the Fmoc-AA loading to 3 equivalents, and lowering the temperature to 75 °C (**Table 1**, entries

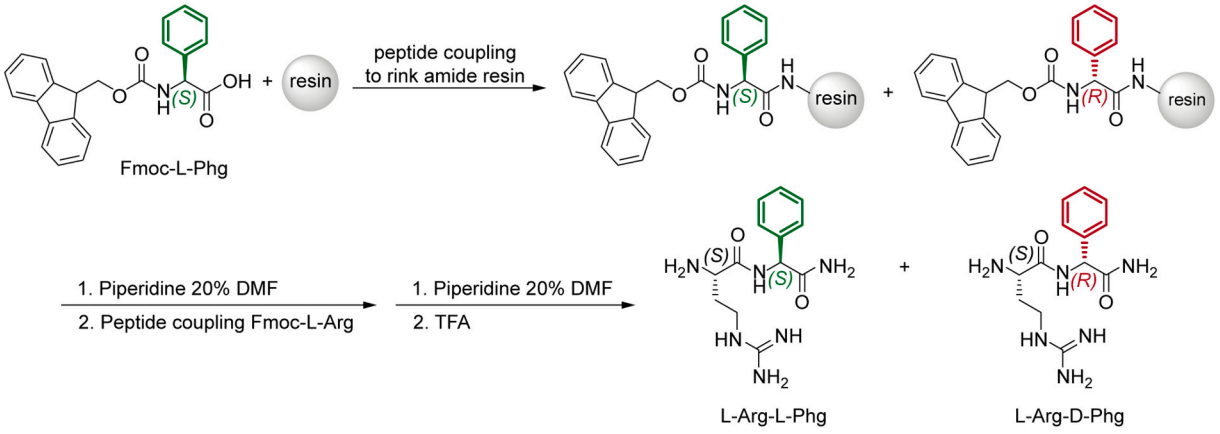

Scheme 1. Fmoc-L-Phg coupling to Rink Amide and elongation with L-Arg to yield dipeptide **1**. The sensitivity of Phg to racemization during its coupling on the resin could lead to epimerization of the final desired dipeptide.

Table 1
Synthesis of dipeptide Arg-Phg (**1**) under different experimental conditions using the proposed instrumental setup. Notes: 'a' = purity determined by HPLC; 'b' = determined on Fmoc-Arg-Phg-NH_2 derivative; 'c' = stereochemical purity (LL/(LD + LL))% determined by NMR integration; 'd' = average of triplicate experiments.

#	Coupling agent	Amino acid eq.	Temperature (°C)	Coupling time (min)	Purity (%)[a,b]	Stereochemical purity NMR (%)[c]
1	HBTU	5	90	5	57	50
2	DIC/Oxyma Pure	5	90	5	>99	>99
3	DIC/Oxyma Pure[d]	5	90	5	>99[d]	>99[d]
4	DIC/Oxyma Pure	5	75	5	97	>99
5	DIC/Oxyma Pure	5	90	3	92	>99
6	DIC/Oxyma Pure	3	90	5	>99	>99

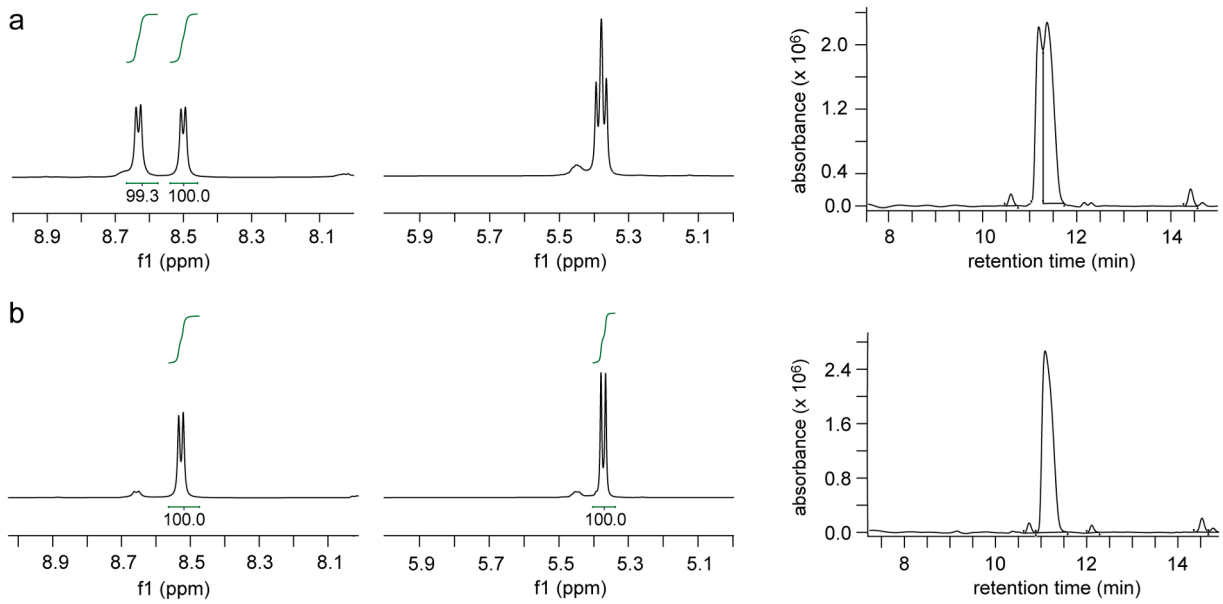

Fig. 1. Comparison of the ^{1}H NMR spectra for the NH (left), CH_α (right) region of Phg residue and HPLC trace of dipeptide Arg-Phg (**1**) synthesized using **a**) HBTU or **b**) DIC/Oxyma Pure.

4–6, **Supplementary figs. 8 and 12**). In all instances, the stereochemical purity of the desired dipeptide **1** remained high (>99%).

Consequently, the conditions detailed in Table 1, entry 2 were selected for the remainder of this study to evaluate the scope and robustness of this methodology on longer sequences, including therapeutic and synthetically challenging linear and cyclic peptides (Fig. 2). We began by synthesising three Phg-containing peptides, ranging from tri- to hexapeptides. The amino acid sequences were selected from the recent literature to serve as benchmarks against state-of-the-art protocols, specifically focusing on challenging substrates prone to epimerization.

As summarized in Table 2 (entries 1 and 2), we examined the synthesis of tripeptide **2** (Ala-Phg-Ile) (**Supplementary figs. 14–20**), a sequence recently synthesized via ball milling [18]. Consistent with our preliminary data, activation using HBTU resulted in significant loss of stereochemical integrity. In contrast, the DIC/Oxyma Pure system effectively suppressed racemization, yielding the stereochemically pure tripeptide **2**. To comprehensively assess the optical purity, the fully deprotected peptides were analyzed as monoprotonated ions via IM-MS. Notably, the extent of epimerization quantified via IM-MS showed excellent correlation with data obtained from HPLC and NMR analysis. The purity of peptide **2** was determined to be >99% by NMR and 94% by IM-MS. This variance is attributed to the different detection limits and physical principles of the two techniques. While the >99% value from NMR may overestimate purity due to minor epimeric signals overlapping with the baseline or major peak shoulders, the higher sensitivity of IM-MS allowed for the detection of the minor epimer. However, the IM-MS integration should be considered primarily diagnostic (or semi-quantitative), as arrival time distributions (ATDs) can be influenced by epimer-specific ionization efficiencies, peak tailing, or gas-phase structural dynamics.

Specifically, the HBTU-mediated synthesis yielded a product mixture exhibiting dual populations in the IM-MS drift time distribution (Fig. 3a), which corroborated the two distinct peaks observed in both the ^{1}H NMR spectrum and HPLC chromatogram. Conversely, the optimized DIC/Oxyma Pure protocol delivered the tripeptide sequence as a single stereoisomer, evidenced by a single doublet ^{1}H NMR resonance (δ 5.56 ppm), a unique drift time distribution in IM-MS analysis, and a single HPLC peak (Fig. 3b). Consequently, tripeptide **2** was obtained with a purity and stereochemical profile comparable to those reported under ball milling conditions [18]. However, the present protocol offers distinct advantages, including a two-fold reduction in coupling reaction times and greater operational simplicity, thereby obviating the need for specialized mechanochemical instrumentation.

Next, we extended the study to the synthesis of pentapeptide **3** (Ala-Val-Pro-Phg-Tyr), a bioactive analogue of the pro-apoptotic sequence H-AVPPhgY-NH_2 that targets the BIR3 domain of XIAP protein [19], which has been previously synthesized via MW-assisted assembly [7]. Our initial attempts using HBTU revealed a significant degree of epimerization (Table 2, entry 3). Conversely, the employment of DIC/Oxyma Pure afforded **3** with excellent stereochemical purity (Fig. 4**a** and **b**) (**Supplementary figs. 21–28**). Notably, this protocol yielded a diastereomeric purity superior to that previously reported for the MW-assisted synthesis using 4-(4,6-dimethoxy-1,3,5-triazin-2-yl)-4-methylmorpholinium tetrafluoroborate (DMTMMBF_4) as coupling agent (71%) [7].

To further assess the robustness of the proposed coupling methodology, we synthesized hexapeptide **4** (Ala-Val-Pro-Phg-Phg-Tyr)

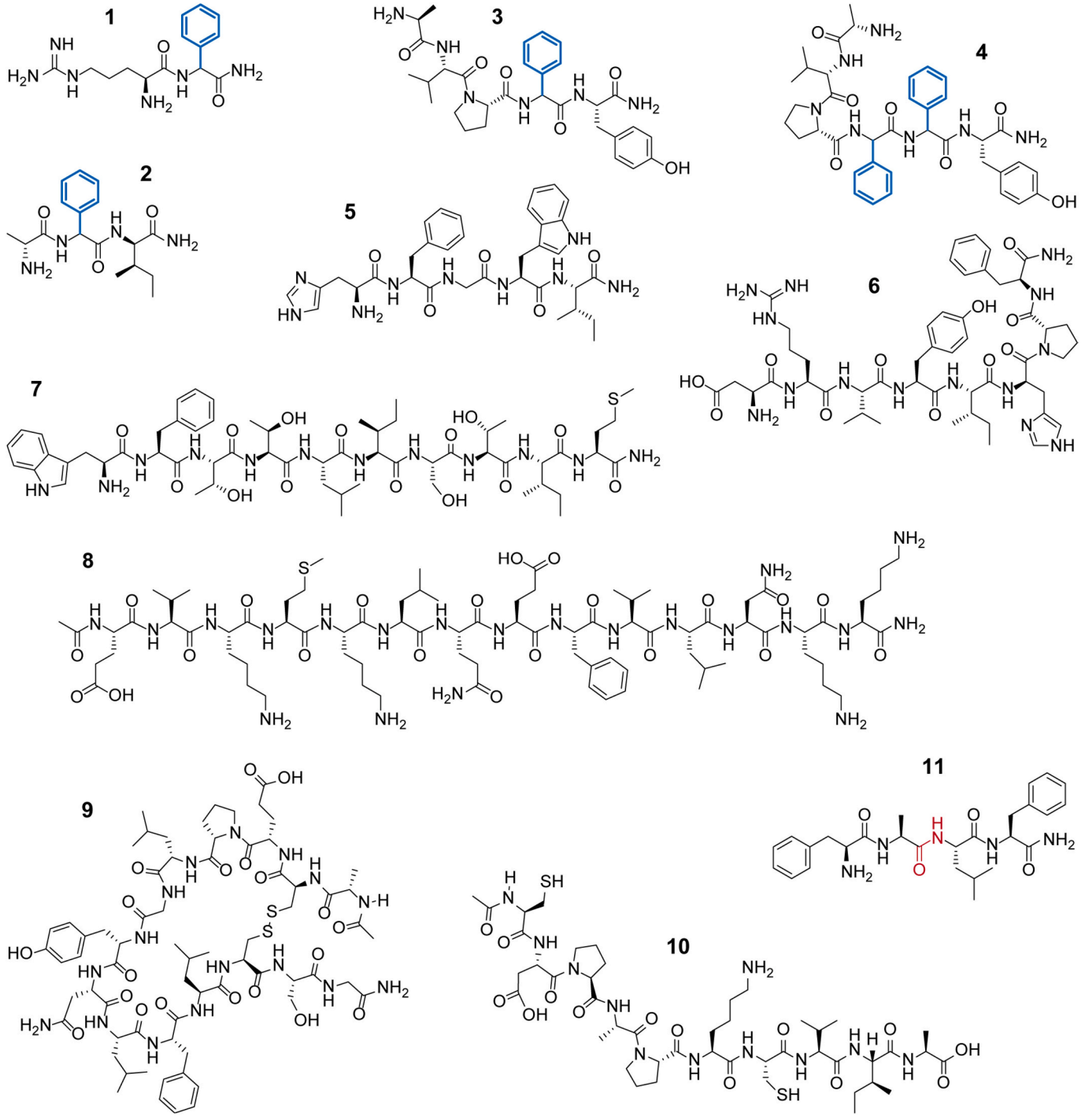

Fig. 2. Molecular structures of the eleven peptides investigated in this study. Phg residues are shown in blue while amide coupling between peptides is shown in red. (For interpretation of the references to colour in this figure legend, the reader is referred to the web version of this article.)

(**Supplementary figs. 29–36**). This sequence represents a significant synthetic challenge due to the presence of two contiguous Phg residues, a motif known to be highly susceptible to Cα-epimerization. As expected, activation with HBTU (Table 2, entry 5) resulted in significant racemization, yielding a complex mixture of four diastereomers. Analysis of the crude ^{1}H NMR spectrum in the region around δ 5.0 ppm revealed that the desired all-L isomer constituted less than 50% of the total population. In marked contrast, the use of DIC/Oxyma Pure (Table 2, entry 6) effectively suppressed epimerization. The ^{1}H NMR spectrum confirmed the presence of the major desired epimer with corresponding two doublets for the two CHα of the Phg residues (**Supplementary fig. 29**). These findings were further corroborated by IM-MS analysis, which confirmed the high diastereomeric purity of the hexapeptide (**Supplementary figs. 35–36**).

Having demonstrated the robustness of our protocol in the synthesis of Phg-containing peptides, we extended the investigation to sequences comprising exclusively proteinogenic amino acids. Specifically, we selected peptide sequences incorporating residues more sensitive to epimerization due to heteroatom-containing side chains [20], as well as sterically demanding sequences characterized by contiguous bulky residues. These distinct challenges were chosen to rigorously assess the general applicability and efficacy of this coupling method.

Table 2
Synthesis Phg-containing peptide sequences: a comparison between HBTU and DIC/Oxyma Pure as coupling agents. Notes: 'a' = purity determined by HPLC; 'b' = determined on Fmoc-deprotected derivative; 'c' = stereochemical purity $((L)_nL)/[((L)_nD) + ((L)_nL)]$% determined by NMR integration; 'd' = stereochemical purity $((L)_nL)/[((L)_nD) + ((L)_nL)]$% determined by IM-MS integration; 'e' = % ratio between the expected peptide and all possible four epimers with different configuration on Phg; n.d. not determined due to peak overlap, see supporting information.

#	Coupling agent	Peptide	Purity (%)[a,b]	Stereochemical purity NMR (%)[c]	Stereochemical purity IM-MS (%)[d]
1	HBTU	Ala-Phg-Ile (**2**)	73	48	36
2	DIC/Oxyma Pure	Ala-Phg-Ile (**2**)	86	>99	94
3	HBTU	Ala-Val-Pro-Phg-Tyr (**3**)	n.d.	59	62
4	DIC/Oxyma Pure	Ala-Val-Pro-Phg-Tyr (**3**)	88	98	97
5	HBTU	Ala-Val-Pro-Phg-Phg-Tyr (**4**)	n.d.	59[e]	33[e]
6	DIC/Oxyma Pure	Ala-Val-Pro-Phg-Phg-Tyr (**4**)	74	90[e]	94[e]

We initially examined the synthesis of pentapeptide **5** (H-His-Phe-Gly-Trp-Ile-NH_2). This sequence features the sterically demanding coupling of Fmoc-L-His(Trt)-OH to an N-terminal phenylalanine (Phe) residue, a transformation notoriously prone to racemization (**Table 3**, entry 1, and Fig. 5a) [21]. Notably, the product was isolated with excellent stereochemical purity. Analysis via 1D and 2D NMR (Fig. 5b and **Supplementary figs. 37–41**), HPLC-MS (**Supplementary fig. 42**) and IM-MS (**Supplementary fig. 43**) revealed a single species, confirming the structural integrity of the pentapeptide. Remarkably, this was achieved with significantly reduced reaction times compared to literature protocols based on fast high-shear overhead mechanical stirring at 700 rpm for 60 min [21].

To further demonstrate the broad applicability of this protocol, we next investigated the synthesis of Angiotensin II (**6**), an octapeptide hormone pivotal in blood pressure regulation [22]. Using the standard DIC/Oxyma Pure coupling system, the peptide sequence **6** (H-Asp-Arg-Val-Tyr-Ile-His-Pro-Phe-NH_2) was obtained with excellent efficiency. Analysis of the crude material revealed a major species characterized by high stereochemical purity (>99%; **Table 3**, entry 2, Fig. 6 and **Supplementary figs. 44–50**). Notably, despite the presence of the aspartic acid (Asp) residue, no evidence of aspartimide-related side reactions was detected [23–25].

To further demonstrate the synthetic utility and robustness of our methodology, we applied the optimized protocol to the synthesis of the Jung-Redemann decapeptide (**7**, H-Trp-Phe-Thr-Thr-Leu-Ile-Ser-Thr-Ile-Met-NH_2). This sequence represents a synthetic benchmark due to the presence of multiple sterically hindered residues and is typically prepared on low-loading resins to mitigate aggregation [26]. Notably, by employing our standard procedure on a commercial high-loading Rink Amide resin, peptide **7** was obtained with high stereochemical integrity, as confirmed by both HPLC spectroscopy and IM-MS analysis (**Supplementary figs. 51–52**). Furthermore, HPLC analysis of the crude material revealed a purity profile superior to those reported in the previous literature [27].

Subsequently, the scope of the method was expanded to the synthesis of the 14-mer HDAC4-derived peptide (**8**) (Ac-Glu-Val-Lys-Met-Lys-Leu-Gln-Glu-Phe-Val-Leu-Asn-Lys-Lys-NH_2), a sequence derived from the binding interface of HDAC4 protein with the transcription factor MEF2D [28]. Specifically, the presence of two glutamic acid (Glu) and four lysine (Lys) residues —amino acids that are susceptible to epimerization [13]—makes peptide **8** a stringent model for validating our synthetic protocol. Indeed, in a peptide sequence of this length, even trace levels of epimerization would generate diastereomeric impurities that are often chromatographically inseparable from the target product. Comprehensive analysis of the crude material by 1D and 2D NMR spectroscopy confirmed the formation of the desired homochiral compound. The stereochemical integrity was further corroborated by IM-MS

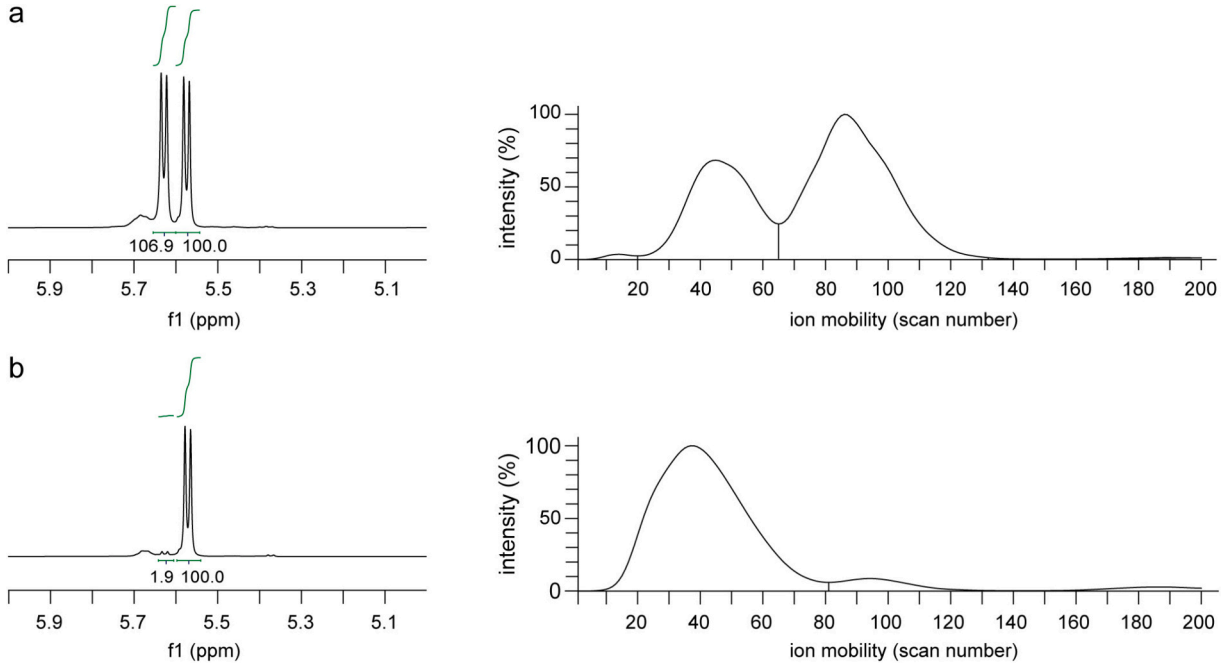

Fig. 3. Comparison of the ^{1}H NMR spectra for the CHα of Phg in tripeptide Ala-Phg-Ile (**2**) and the corresponding IM-MS profile obtained using **a**) HBTU or **b**) DIC/Oxyma Pure.

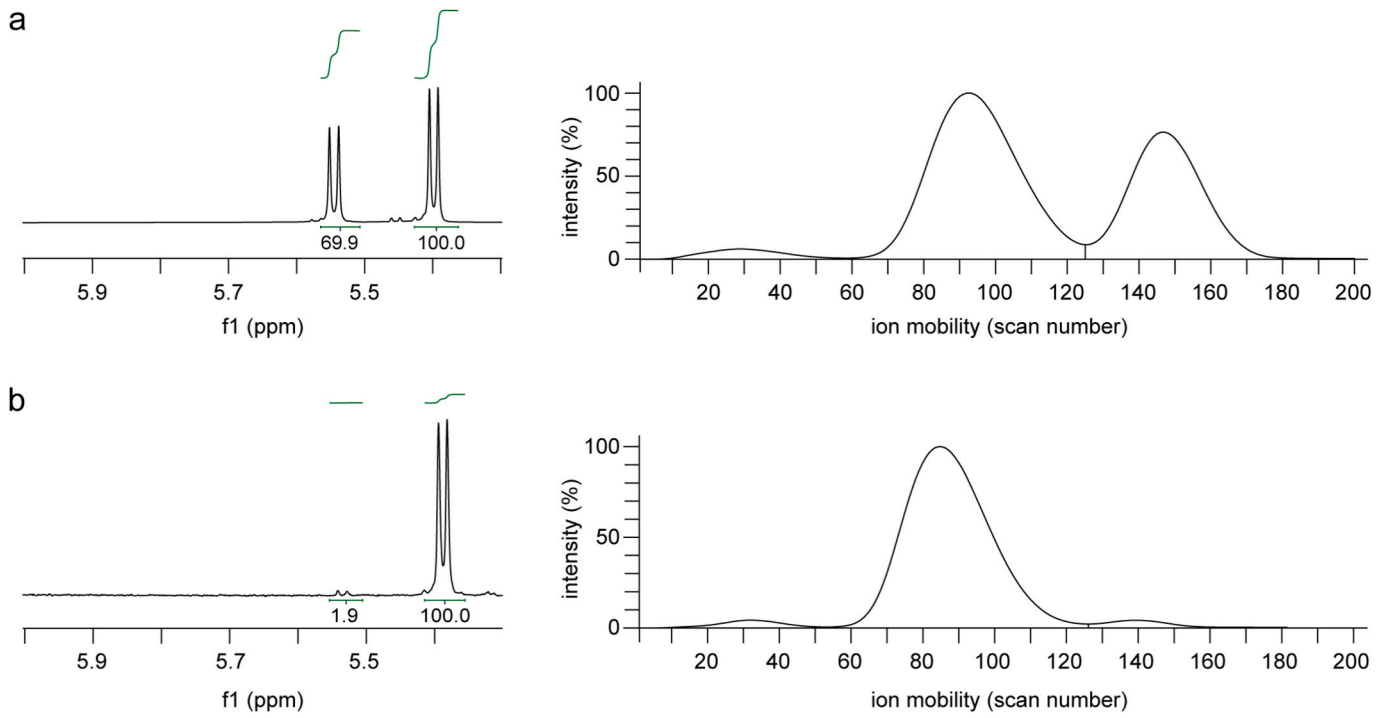

Fig. 4. Comparison of the ^{1}H NMR spectra for the CH_{α} of Phg in pentapeptide Ala-Val-Pro-Phg-Tyr (**3**) and corresponding IM-MS profile obtained using **a**) HBTU or **b**) DIC/Oxyma Pure.

Table 3
Synthesis of different peptide sequences comprising exclusively proteinogenic amino acids. Notes: 'a' = determined by HPLC analysis; 'b' = determined on Fmoc-deprotected derivative; 'c' = stereochemical purity $((L)_nL)/[((L)_nD) + ((L)_nL)]$% determined by NMR integration; 'd' = stereochemical purity $((L)_nL)/[((L)_nD) + ((L)_nL)]$% determined by IM-MS integration; 'e' =cyclic peptide formed via disulfide bonding between the underlined cysteine residues; 'f' = see **Supplementary fig. 66**.

#	Peptide sequence	Purity (%)[a,b]	Stereochemical purity NMR (%)[c]	Stereochemical purity IM-MS (%)[d]
1	H-His-Phe-Gly-Trp-Ile-NH_2 (**5**)	84	>99	>99
2	H-Asp-Arg-Val-Tyr-Ile-His-Pro-Phe NH_2 (angiotensin II, **6**)	69	>99	>99
3	Ac-Glu-Val-Lys-Met-Lys-Leu-Gln-Glu-Phe-Val-Leu-Asn-Lys-Lys-NH_2 (pHDAC4, **8**)	88	>99	>99
4	Ac-Ala-Cys-Glu-Pro-Leu-Gly-Tyr-Asn-Leu-Phe-Leu-Cys-Ser-Gly-NH_2 (**9**)[e]	86	>99	n.d.[f]
5	Ac-Cys-Asp-Pro-Ala-Pro-Lys-Cys-Val-Ile-Ala-NH_2 (**10**)	91	>99	>99

analysis, which revealed negligible formation of epimers (**Table 3**, entry 3 and **Supplementary figs. 53–59**).

Next, we determined the half-maximum inhibitory concentration (IC_{50}) of peptide **8**–synthesized via both the standard room-temperature (RT) protocol and our high-temperature (HT) method–toward the MEF2D protein. To this end, we employed a fluorescence polarization (FP)-based competition assay to examine the ability of the two unlabelled peptides to antagonize the interaction between a fluo-pHDAC4 probe and MEF2D [28]. The assay revealed that both versions of peptide **8** displaced the probe in a dose-dependent manner, yielding comparable IC_{50} values of 7.8 μM (RT SPPS) and 6.8 μM (HT SPPS), respectively (Fig. 7a). Collectively, these functional insights demonstrate that our protocol successfully generates biochemically active molecules, providing a crucial biological validation that complements standard analytical purity metrics.

To further challenge the applicability of our methodology, we next explored the synthesis of the disulfide-tethered 14-mer peptide **9** (H-Ala-Cys-Glu-Pro-Leu-Gly-Phe-Asn-Arg-Trp-Ile-Cys-Ser-Gly-NH_2), a macrocyclic peptide inhibitor of ACE2 enzyme [29]. Peptide **9** was successfully obtained under our optimized conditions, maintaining high purity and stereochemical integrity (**Supplementary 60–66**). To evaluate its functional activity, we determined the inhibitory constant (K_i) of peptide **9**–synthesized via both the standard RT protocol and our HT method–toward the ACE2 protein. To this end, we monitored the residual activity of the hACE2 enzyme in the presence of a fluorogenic substrate and varying concentrations of each peptide at physiological pH and at room temperature. The study revealed that both versions of peptide **9** retained strong inhibitory potencies, yielding comparable K_i values of 1.8 nM (RT) and 2.2 nM (HT), respectively (Fig. 7b) thus further demonstrating the capability of our approach to deliver biochemically active molecules.

Next, we evaluated the generality of the protocol with respect to the use of different solid support. To this end, we performed the synthesis of decapeptide **10** (Ac-Cys-Asp-Pro-Ala-Pro-Lys-Cys-Val-Ile-Ala-COOH) on a 2-chlorotrityl chloride (2-CTC) resin and compared the results to those obtained using a standard Rink Amide resin. 1D, 2D NMR and IM-MS analyses revealed that decapeptide **10** was obtained with a purity and stereochemical integrity comparable to the Rink Amide-derived product (**Supplementary figs. 67–73**). These results demonstrate that this methodology is not restricted to Rink Amide supports and can be successfully extended to alternative solid supports without compromising performance.

To further extend the scope of our methodology beyond stepwise Fmoc-SPPS, we subsequently investigated peptide fragment condensation. It is well established that the activation of a peptide C-terminal

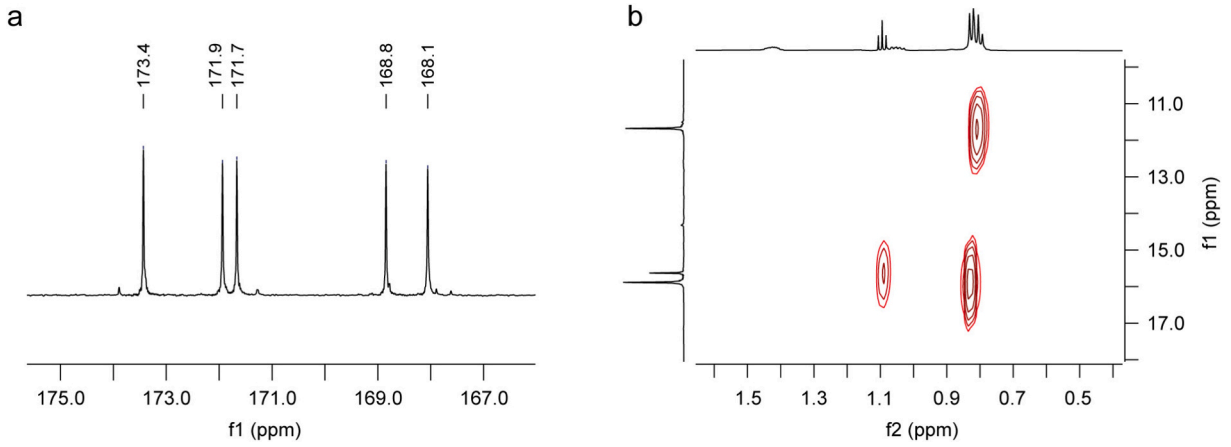

Fig. 5. a) $^{13}C\{^{1}H\}$ NMR spectrum of the region of the carbonyl residues for the pentapeptide **5** (H-His-Phe-Gly-Trp-Ile-NH_2) showing five major resonances; **b**) Portion of the HSQC spectrum of the pentapeptide **5** showing the presence of just one Ile set of resonances for the two methyl units in the side chain of the amino acid (cross-peak at ^{1}H 1.09 ppm and $^{13}C\{^{1}H\}$ at 15.6 ppm corresponds to diethyl ether traces).

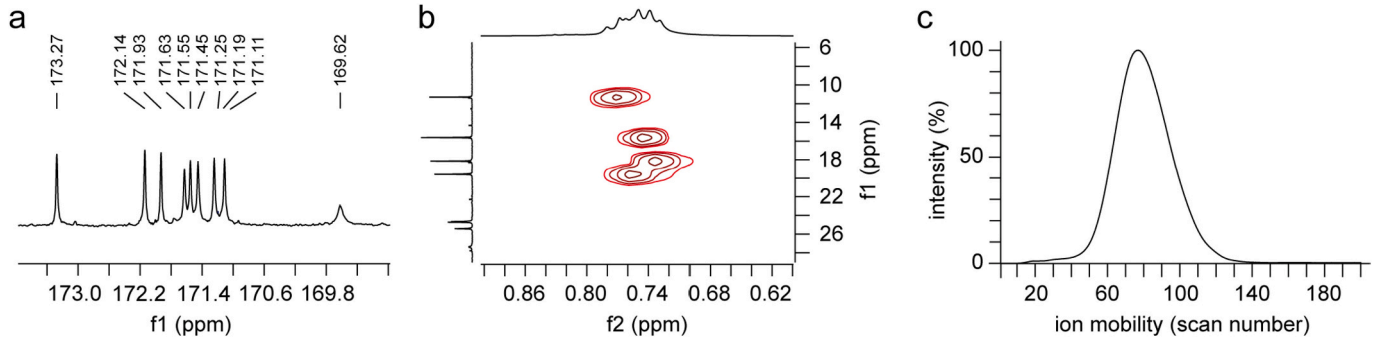

Fig. 6. a) $^{13}C\{^{1}H\}$ NMR spectrum of the region of the carbonyl residues for the octapeptide Fmoc-Angiotensin II (**6**) showing nine major resonances; **b**) Portion of the HSQC spectrum of Fmoc-Angiotensin II (**6**) showing the presence of only four cross-peaks for the four diastereotopic methyl units in the side chains of Val and Ile; **c**) IM-MS of H-Angiotensin II.

carboxylic moiety carries a significantly higher risk of epimerization compared to a single Fmoc-amino acid. This is primarily due to the increased acidity of the Cα-proton and the propensity to form oxazolone intermediates (**Supplementary fig. 74**). To evaluate our protocol in this challenging context, we designed the convergent synthesis of tetrapeptide **11** (H-Phe-Ala-Leu-Phe-NH_2) via the coupling of the protected dipeptide Fmoc-Phe-Ala-OH to the resin-bound H-Leu-Phe-resin. IM-MS analysis of the crude product revealed a single drift time distribution (**Supplementary fig. 75**), unequivocally confirming the stereochemical robustness of the DIC/Oxyma Pure coupling system.

Although recent strategies to minimize protecting group manipulations have shown promise [27,30], SPPS remains burdened by substantial waste generation. To evaluate the environmental sustainability of our proposed methodology [31], we determined the Process Mass Intensity (PMI) for the optimized DIC/Oxyma Pure protocol, in alignment with contemporary green synthesis metrics [32,33]. PMI calculation for peptide **8** with a molecular weight of 1774 Da revealed a cumulative PMI value of approximately 2993 (**Supplementary fig. 76**). This translates to an average PMI of 200 per amino acid coupling cycle. Notably, these data represent a significant improvement over standard benchmarks corresponding to an average of PMI in the range 870–1460 per amino acid [32]. As anticipated, the breakdown of the PMI contributions indicates that solvent usage remains the primary factor; however, the impact is more pronounced in the workup and precipitation phases rather than during the synthesis and washing steps.

Finally, driven by the imperative to replace DMF [34] with more sustainable alternatives [35], we investigated the synthesis of the model dipeptide H-Arg-Phg-NH_2 **1** (Table 1) using DIC/Oxyma Pure in binary solvent mixtures. Toward this goal, we evaluated DMSO:*i*PrOH [36] (75:25v/v) and anisole:DMC [37] (70:30 v/v) at elevated temperatures of 75 °C and 88 °C, respectively, to optimize coupling efficiency. In both instances, dipeptide **1** was obtained with excellent stereochemical fidelity (>99%), confirmed by the presence of a single doublet for the Phg Cα proton in the ^{1}H NMR spectra (**Supplementary fig. 9**). Furthermore, inspired by recent work from Albericio and colleagues on aqueous SPPS [38], we adapted our protocol to a H_2O:*i*PrOH (60:40 v/v) system using a hydrophilic TentaGel resin at 75 °C. This aqueous medium also yielded the dipeptide **1** with high stereochemical purity (>99%, determined by ^{1}H NMR (**Supplementary fig. 9**)). While diastereomeric excess remained consistently high across all media, HPLC analysis of the crude products revealed varying purities of 52%, 56%, and 62% for the anisole:DMC, DMSO:*i*PrOH, and H_2O:*i*PrOH solvent systems, respectively (**Supplementary fig. 13**). Collectively, these results validate the versatility of the proposed instrumental set-up, demonstrating its applicability to a broad range of green solvent systems, even though the use of DMF provides better purity profiles.

3. Conclusions

In this study, we have established a robust and accessible SPPS methodology that enables the synthesis of peptides with high purity, abbreviated reaction times, and minimal waste generation using standard laboratory equipment. In Table 4 are reported for comparison other instrumental systems for SPPS which represent standard

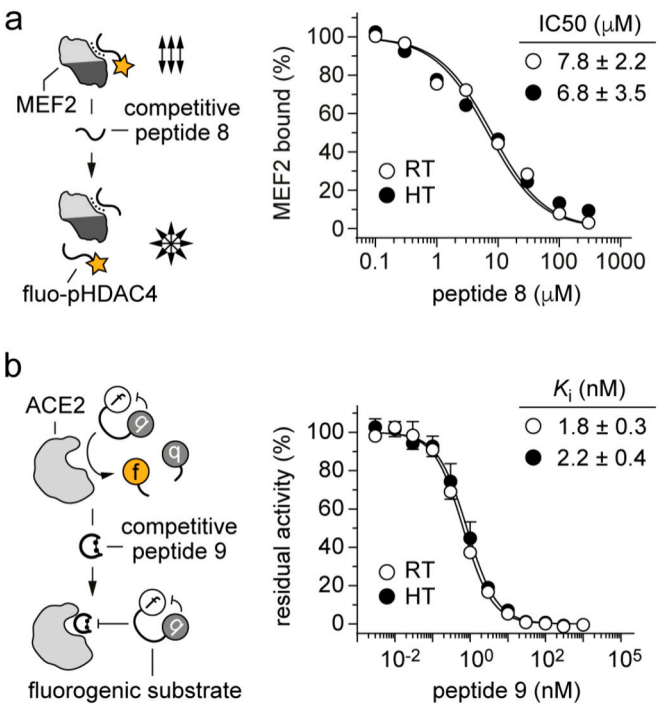

Fig. 7. Functional comparison of peptides obtained under standard room-temperature (RT) protocol and high-temperature (HT) SPPS conditions. **a)** Fluorescence polarization competition assay showing displacement of a fluorescein-labelled pHDAC4 peptide (fluo-pHDAC4) from MEF2D by the peptide **8** obtained via both RT and HT protocols. The indicated IC50 values are the results of three independent experiments and are presented as mean (dots) ± s.d. (bars); **b)** Enzymatic inhibitory activity of the macrocyclic peptide **9** against ACE2, reported as residual enzymatic activity as a function of the concentration macrocyclic inhibitor **9** obtained via both RT and HT methods. The indicated K_i values are the results of two independent experiments and are presented as mean (dots) ± s.d. (bars).

benchmarks in terms of performance, efficiency and the relative economic investment requested.

The protocol demonstrated broad applicability across a diverse range of sequences, including those containing residues prone to epimerization (e.g., Phg) and hindered amino acids requiring challenging couplings. Notably, the use of the DIC/Oxyma Pure coupling system at 90 °C maintained exceptional stereochemical integrity, a result corroborated by a comprehensive analytical suite including 1D and 2D NMR, IM-MS, and HPLC. Although this method yielded a low average PMI, it has been tested primarily using DMF and should be viewed solely as a first step toward a greener solution. Indeed, although compatible with emerging sustainable binary solvent mixtures, DMF still delivers better performance than some of the eco-friendly alternatives tested. Further studies are therefore necessary to fully support a transition toward more sustainable peptide synthesis [40].

Despite these promising results, the methodology requires further investigation. To date, our study has focused exclusively on sequences shorter than fifteen amino acids, primarily incorporating Phg and standard natural amino acids. To fully establish the broad applicability of this method, future efforts must explore more structurally diverse and complex molecules, such as peptides sequences exceeding twenty residues, bicyclic peptides, post-translationally modified peptides, and 'difficult-to-synthesize' hydrophobic sequences or sequences bearing aggregating motifs. Each of these classes introduces unique physicochemical challenges, such as altered solubility, complex gas-phase behavior, or heightened conformational flexibility, that will require further optimization. Furthermore, while the protocol has demonstrated compatibility with Rink-Amide, TentaGel and 2-CTC resins, its performance on additional commonly utilized SPPS supports remains to be verified. Expanding the utility of this method to these more challenging peptide sequences represents a logical next step and is currently the subject of ongoing investigation in our laboratory.

From a sustainability perspective, although our methodology is focused on an instrumental optimization, further studies validating a broader repertoire of sustainable solvents, minimizing amino acid equivalents, lowering piperidine concentrations for Fmoc deprotection, and optimizing the DMF in the washing steps are advisable.

Finally, regarding engineering and scalability, studies are underway to evaluate compatibility with automated synthesizers and iterative peptide synthesis workflows. As the current work was conducted at the milligram scale (10–100 mg), scaling up to gram-scale synthesis will require solving technical bottlenecks—such as uneven heating and mass transfer limitations—to ensure industrial viability. Addressing these challenges will allow a more comprehensive comparative evaluation of our protocol against current state-of-the-art microwave-assisted and room-temperature automated synthesizers.

4. Experimental section

4.1. General

Materials and methods: Fmoc-protected amino acids, Fmoc-rink amide MBHA resin (100–200 mesh, loading 0.4–0.9 mmol/g resin, 0.01 mmol scale), TentaGel resin (loading 0.23 mmol/g resin), *N*,*N*-dimethylformamide (DMF) was purchased from Novabiochem (Darmstadt, Germany). Acetonitrile (ACN), formic acid, trifluoroacetic acid

Table 4
Comparison between the proposed method and existing rapid SPPS techniques, such as microwave-assisted and ball-milling methods. Evaluated parameters include equipment requirements, reaction temperature, coupling time, peptide scale, crude purity, and stereochemical purity. Notes: 'n.a.' = not available; '#' = average of multiple peptide syntheses.

	SPPS methodology			
	Microwave-assisted	Ball-milling	Automated SPPS	Syringe-based heating
Equipment requirements	Microwave (The Liberty™)	Retsch Mixer Mill 200 or 400	Pure Prep® Chorus synthesizer	Fig. S1
Reaction temperature	50 °C or 75 °C	33 °C	90 °C	90 °C
Coupling time	10 min	10 min	2 min	3 or 5 min
Peptide scale	0.025–1.0 mmol	0.049 mmol	0.100 mmol	0.065 mmol
Crude purity[a]	n.a.	87%	85%	92%
Stereochemical purity[a]	63% by RP-HPLC (with HBTU or DMTMM-Cl or DMTMM-BF or HBTU/HOBT as coupling agents)	>99% (with EDC HCl/Oxyma Pure as coupling agents)	95% RP-HPLC (with DIC/Oxyma Pure as coupling agents)	98% by NMR 97% by IM-MS (with DIC/Oxyma Pure as coupling agents)
Price	60.000–110.000 $	5.000–15.000 $	50.000–100.000 $	<500 $
References	[7]	[8]	[39]	Present work

(TFA), diethyl ether, dichloromethane (DCM), tris-isopropylsilane (TIS), piperidine, N,N-diisopropylethylamine (DIPEA), and dimethyl sulfoxide (DMSO) were purchased from Merck (Darmstadt, Germany). *N*,*N*,*N*′,*N*′-Tetramethyl-O-(1H-benzotriazol-1-yl)uronium hexafluorophosphate (HBTU) was purchased from ChemPep (Wellington, FL, USA). All chemicals were used as received without further purification. All other reagents such as dipeptide Phe-Ala and Fmoc-OSu used for synthesis as well as $CDCl_3$ (99.8%, stabilized with silver foil) and DMSO-d_6 were purchased from Merck (Darmstadt, Germany) with the highest commercially available purity and employed without further treatment. Fmoc-Phe-Ala was synthesized starting from Phe-Ala by reacting it with the Fmoc-Osu as previously described [41]. Transfer of liquids with a volume ranging from 1 to 10 μL or from 10 to 100 μL was performed using a Microman M1 pipette (Gilson, systematic error: 1.40–1.60%) equipped with 10 or 100 μL pipette tips respectively. The weighing of substrates and products was performed using a Dhaus Pioneer balance.

4.2. General procedure for solid-phase peptide synthesis

Peptide synthesis was carried out manually in polypropylene syringes that were fitted with a porous polyethylene disc containing a magnetic stirring bar loaded with resin beads and inserted in the aluminium manifold. The Fmoc group was removed with piperidine/DMF (1:4 *v*/v; 3 mL × 1 × 1 min at 90 °C with shaking at 300 rpm). Washing between the deprotection, coupling, and final deprotection steps was carried out using DMF (3 mL × 3). The deprotection step was carried out using a 20% v/v solution of piperidine in DMF for (3 mL × 1 × 1 min at 90 °C with shaking at 300 rpm). The amino acid coupling was carried out (1 × 5 min at 90 °C) for each Fmoc-amino acid using Oxyma Pure coupling mixture (5 eq. amino acid, 5 eq. Oxyma Pure and 5 eq. DIC solution in DMF 5 mL) with shaking at 300 rpm. Washes in between couplings were performed using DMF (2.5 mL × 3). To ensure continuous and accurate monitoring of the internal temperature of the heating setup, an external digital thermometer probe was placed directly inside a control reaction vessel. This control vessel contained the solvent-swollen resin bed under standard operational conditions. Calibration confirmed that the internal temperature increased progressively before reaching the setup temperature equilibrium within one minute. To control solvent evaporation, the reaction syringe was tightly sealed using a specialized cap. Because this created an effectively closed system, any solvent vaporized during the 90 °C heating cycle condensed on the cooler upper walls of the syringe barrel and returned to the reaction mixture (reflux effect), thereby preventing solvent loss. The duration of the heating cycles was strictly monitored and controlled using a digital timer. Uniform resin suspension was maintained via magnetic stirring and verified through continuous visual inspection. This ensured that the resin bed remained fluid and uniform throughout the reaction. At the end of the synthetic process, washes were performed with DCM (3 mL × 3). The final peptides were deprotected and cleaved from the resin under reducing conditions using a TFA/H_2O/TIS mixture (95:2.5:2.5% *v*/v) for 2.5 h at room temperature with shaking at 300 rpm. The resin was removed by vacuum filtration, and the peptides were precipitated with cold diethyl ether (7 mL × 1 h) and centrifuged at 5000 rpm for 5 min at 4 °C on a Heraeus Multifuge X1R centrifuge (Thermo Fisher Scientific, Waltham, MA, USA) under inert atmosphere. The precipitated linear peptides were washed twice with cold diethyl ether (6.5 mL × 2) to remove TFA.

4.2.1. High performance liquid chromatography analyses

The purity and molecular mass of each peptide was determined on the fully deprotected derivative, or the Fmoc protected derivative for highly hydrophilic peptides, by electrospray ionization mass spectrometry (ESI-MS) performed on a Waters ZQ mass spectrometer with separation module Waters 2695, UV-VIS detector Waters 2489. The system operated with the standard ESI source and in the positive ionization mode. Peptides were dissolved in ACN:H_2O (50:50% *v*/v) solution at a final concentration of 0.5 mg/mL and run at flow rate of 0.8 mL/min with the following gradient: 10% of eluent B from 0 to 3 min, linear gradient up to 90% B from 3 to 15 min 100% B from 15 to 18 min and 10% B from 18 to 19 min (eluent A: 99.9% v/v H_2O, 0.1% v/v formic acid; eluent B: 99.9% v/v ACN, 0.1% v/v formic acid). The reversed-phase HPLC column was a XTerra MS C18 (3.5 μm, 4.6 × 150 mm) from Waters (Milford, MA, USA). Absorbance was monitored at 220 and 280 nm (AU). Data were acquired, processed, and analyzed using the and MNova software (Mestrelab Research, Santiago de Compostela, Spain).

4.3. Nuclear magnetic resonance analyses

All nuclear magnetic resonance (NMR) experiments were performed on a Bruker Advance operating at 400 MHz equipped with a direct observe 5-mm BBFO FB probe with a self-shielded z-gradient and a Bruker 600 NEO with cryo-probe Prodigy operating with liquid nitrogen operating at 600 MHz equipped with an inverse cryo-probe. The experiments were performed at 300 K and the temperature was calibrated using a water standard showing accuracy within ±0.2 K. Chemical shifts of ^{1}H NMR and $^{13}C\{^1H\}$ NMR are given in ppm and refer to $SiMe_4$ (TMS) as standard. The proton signal of the deuterated solvent was used as reference: $CDCl_3$ δ ^{1}H = 7.26 ppm, δ $^{13}C\{^1H\}$ = 77.16 ppm; DMSO δ ^{1}H = 2.05 ppm. Coupling constants (*J*) are reported in Hertz (Hz). Standard abbreviations indicating multiplicity were used as follows: s (singlet), d (doublet), dd (doublet of doublets), m (multiplet).

4.4. Ion mobility mass spectroscopy analyses

Ion mobility experiments were performed via direct infusion using a high-resolution mass spectrometer coupled with a cyclic ion mobility (cIM) device (Select Series Cyclic IMS, Waters Corporation, Wilmslow, UK). Unlike traditional linear drift-tube instruments, the cyclic geometry allows for the extension of the ion separation path through multiple passes (cyclic reiteration) within the drift region. This architecture significantly increases the separation path length, enabling high-resolution results unattainable with conventional systems. To ensure the complete resolution of epimers and avoid signal overlap, the separation was carried out using more than 10 passes, theoretically extending the drift tube length by a factor of approximately 10. The key operating parameters adopted were cyclic traveling wave (TW) velocity of 375 m/s; array TW velocity of 375 m/s; TW static height of 15 V; TW ramp start height of 15 V; TW ramp end height of 35 V, TW ramping rate of 2.5 V/ms; push per bin of 2; number of bins of 200. To optimize experimental conditions, the quadrupole mass filter was set to isolate the specific *m/z* of interest. Concurrently, the injection flow rate and pDRE attenuation were adjusted to achieve a target ion intensity of approximately 1×10^5

4.5. ***Determination of enzymatic inhibitory activity***

The inhibitory activity of the macrocyclic peptide **9**–synthesized via both the standard RT protocol and our HT method–was assessed by monitoring the residual activity of human ACE2 enzyme in the presence of a fluorogenic substrate and different concentrations of peptide **9**. The activity assay was performed by incubating 0.25 nM of hACE2 with 50 μM fluorogenic substrate Mca-Ala-Pro-Lys(Dnp) − OH (MedChemExpress, Monmouth Junction, NJ, USA) and 3-fold peptide dilutions (ranging from 0.03 nM to 100 μM). Macrocyclic peptide **9**, synthesized via both the standard RT protocol and our HT method, possessed comparable final purity. All reagents were diluted in 10 mM Tris−HCl, pH 7.4, 300 mM NaCl, 100 μM ZnCl2, 0.1% *w*/*v* BSA, and 0.1% DMSO assay buffer. The measurements were performed on a Victor Nivo Multimode microplate reader (Revvity, Buckinghamshire, United Kingdom) using black flat-bottom 96-well OptiPlate microplates (Revvity, Buckinghamshire, United Kingdom). The enzymatic reactions were

performed at 25 °C for 90 min, under shaking with a maximum excitation wavelength (λ_{ex}) of 320 nm and maximum emission wavelength (λ_{em}) of 405 nm. The initial velocities were monitored as changes in fluorescence intensity. Half-maximum inhibitory concentration (IC50) values were determined using GraphPad Prism v8.2.1 software. The inhibitory constant (K_i) values were subsequently calculated using the Cheng-Prusoff equation:

$$K_i = \frac{IC_{50}}{1 + \frac{[S]}{K_m}}$$

where [S] is the concentration of the Mca-Ala-Pro-Lys(Dnp)-OH substrate, and K_m (17 μM) is the Michaelis−Menten constant for the same fluorogenic substrate hydrolysed by hACE2, which has been determined by standard Michaelis−Menten equations as previously described [29].

4.6. Fluorescence polarization competitive binding assays

Protein binding by peptide **8** – synthesized via both the standard room-temperature (RT) protocol and our high-temperature (HT) method – was measured by incubating different concentrations of unlabelled peptide **8** ligand ranging from 0.1 to 300 μM with 0.26 μM fluo-pHDAC4 and 20 μM of MEF2D. Peptide **9**, synthesized via both the standard RT protocol and our HT method, possessed comparable final purity. Each mixture (100 μL) containing 10 mM HEPES, 200 mM NaCl, 1 mM DTT, 1 mM EDTA, pH 7.7, 0.26 μM fluo-pHDAC4, 20 μM of protein and the peptide **8** was transferred into black 96-well OptiPlate microplates (Revvity, Buckinghamshire, United Kingdom) and incubated at room temperature for 1 h. Fluorescence polarization signals were recorded at 25 °C using a Victor Nivo Multimode microplate reader (Revvity, Buckinghamshire, United Kingdom) equipped with a 480 nm excitation filter, a 535 nm emission filter, and a 505 nm dichroic mirror. Orbital shaking was applied (200 rpm for 0.1 s). Controls samples without proteins and without peptide ligands were also prepared to estimate fluorescence of displaced and bound probe, respectively. The average fluorescence polarization values of at least three independent experiments were plotted as a function of peptide ligand concentration. Half-maximum inhibitory concentration (IC50) values were determined using GraphPad Prism v8.2.1 software.

The half maximal inhibitory concentration of each molecule was calculated applying the following equation:

$$F = F_L + \frac{(F_{LP} - F_L)_x}{1 + \frac{I}{IC_{50}}}$$

where F is the measured average fluorescence polarization, F_L is the fluorescence polarization of free labelled peptide, F_{LP} is the maximum fluorescence polarization of the peptide-protein complex, and I is the concentration of the compound.

Declaration of use of generative AI and AI-assisted technologies in the writing process

During the preparation of this work, the authors used Gemini as aids in text editing (but not to generate text). After using this tool/service, the authors reviewed and edited the content as needed and take full responsibility for the content of the published article.

CRediT authorship contribution statement

Giacomo Bettin: Writing – review & editing, Writing – original draft, Visualization, Investigation, Formal analysis, Data curation, Conceptualization. **Matilde Salvadoretti:** Writing – review & editing, Writing – original draft, Visualization, Investigation, Formal analysis, Data curation. **Guglielmo Rossi:** Formal analysis. **Fabrizio Fabris:** Writing – review & editing, Supervision, Investigation. **Alessandro Bonetto:** Formal analysis, Data curation. **Claudio Brancolini:** Writing – review & editing, Supervision. **Alessandro Scarso:** Writing – review & editing, Writing – original draft, Supervision, Investigation. **Alessandro Angelini:** Writing – review & editing, Supervision, Investigation, Funding acquisition.

Funding sources

This material is based upon work supported by the 'Veneto Regional Programme European Social Fund Plus' ('PR VENETO FSE+ 2021–2027'), project code 2120–0012–553-2023 - CUP H77G23000140002 (to G.B., A.S. and A.A.), the National Recovery and Resilience Plan (PNRR) and the European Union – Next Generation-EU as part of the research program "National Centre for Gene Therapy and Drugs based on RNA Technology" CUP E63C22000940007 under the project ALLIANCE – CUP H73C24000120005 (to M.S., F.F., A.A. and A.S.), the National Recovery and Resilience Plan (PNRR) – Next Generation-EU and the Ministry of University and Research (MUR) of Italy – ministerial decree No. 630/2024, M4 C2 Inv. 3.3 CUP G23C24001310005 (to G.B.), and the Ministry of University and Research (MUR) of Italy, D.M. 1274/2021 "Programma d'efficientamento tecnologico-prestazionale del Campus scientifico dell'Università Ca' Foscari Venezia" (CUP H77G22000040004).

Declaration of competing interest

The authors declare the following financial interests/personal relationships which may be considered as potential competing interests: Alessandro Angelini reports a relationship with Arzanya S.r.l. that includes: board membership. If there are other authors, they declare that they have no known competing financial interests or personal relationships that could have appeared to influence the work reported in this paper.

Acknowledgements

The authors would like to thank Dr. Giuseppe Borsato for technical assistance with peptide purification and mass spectrometry analysis. The authors are grateful to all the group members for helpful discussions and for critical reading of this manuscript.

Appendix A. Supplementary data

Supplementary data to this article can be found online at https://doi.org/10.1016/j.bioorg.2026.110323.

Data availability

Data will be made available on request.

References

[1] D. Sharma, I. Dhiman, S. Das, D.K. Das, D.D. Pramanik, S.K. Dash, A. Pramanik, Recent advances in therapeutic peptides: innovations and applications in treating infections and diseases, ACS Omega 10 (2025) 17087–17107, https://doi.org/10.1021/acsomega.5c02077.
[2] Z. Zhang, J. Gao, L. Yuan, B. Duan, H. Yang, L. Ma, K. Lu, Self-assembling peptide hydrogels: design, mechanisms, characterization, and biomedical applications, Soft Matter 21 (2025) 4771–4791, https://doi.org/10.1039/d5sm00396b.
[3] T.H.R. Kuster, T. Schnitzer, Peptide catalysis: trends and opportunities, Chem Catalysis 5 (2025) 101339, https://doi.org/10.1016/j.checat.2025.101339.
[4] M. Wang, H. Xia, C. Wang, T. Zhang, M. Zhang, X. Li, C. Peng, T. Jing, Y. Wang, L. Peng, P. Wang, From precision synthesis to cross-industry applications: the future of emerging peptide technologies, Pharm. Res. 218 (2025) 107839, https://doi.org/10.1016/j.phrs.2025.107839.
[5] S.B.H. Kent, Fundamental aspects of SPPS and green chemical peptide synthesis, J. Pept. Sci. 31 (2025) e70013, https://doi.org/10.1002/psc.70013.
[6] L. Ferrazzano, D. Corbisiero, M. Catani, A. Cavazzini, G. Martelli, P. Cantelmi, T. Fantoni, A. Mattellone, C. De Luca, S. Felletti, W. Cabri, A. Tolomelli, Sustainability in peptide chemistry: current synthesis and purification technologies

and future challenges, Green Chem. 24 (2022) 975–1020, https://doi.org/10.1039/D1GC04387K.
[7] M.A. Elsawy, C. Hewage, B. Walker, Racemisation of *N*-Fmoc phenylglycine under mild microwave-SPPS and conventional stepwise SPPS conditions: attempts to develop strategies for overcoming this, J. Pept. Sci. 18 (2012) 302–311, https://doi.org/10.1002/psc.2398.
[8] a) Y. Yeboue, N. Rguioueg, G. Subra, J. Martinez, F. Lamaty, T.-X. Métro, Gram-scale synthesis of a hexapeptide by fragment coupling in a ball mill, Eur. J. Org. Chem. (2022) e202100839, https://doi.org/10.1002/ejoc.202100839;
b) O. Maurin, P. Verdié, G. Subra, F. Lamaty, J. Martinez, T.-X. Métro, Peptide synthesis: ball-milling, in solution, or on solid support, what is the best strategy? Beilstein J. Org. Chem. 13 (2017) 2087–2093, https://doi.org/10.3762/bjoc.13.206.
[9] A. Wróblewska, I.I. Bak-Sypien, P. Paluch, E. Wielgus, J. Zając, A. Jeziorna, S. Kaźmierski, M.J. Potrzebowski, Solvent-free Mechanosynthesis of oligopeptides by coupling peptide segments of different lengths – elucidating the role of cesium carbonate in ball mill processes, Chem. A Eur. J. 30 (2024) e202400177, https://doi.org/10.1002/chem.202400177.
[10] a O. Flögel, J.D.C. Codée, D. Seebach, P.H. Seeberger, Microreactor Synthesis of β-Peptides, Angew. Chem., Int. Ed. 45 (2006) 7000–7003, https://doi.org/10.1002/anie.200602167;
b) E.T. Sletten, J. Danglad-Flores, M. Nuño, D. Guthrie, P.H. Seeberger, Automated Glycan Assembly in a Variable-Bed Flow Reactor Provides Insights into Oligosaccharide–Resin Interactions, Org. Lett. 22 (2020) 4213–4216, https://doi.org/10.1021/acs.orglett.0c01264.
[11] J.N. Naoum, I. Alshanski, G. Mayer, P. Strauss, M. Hurevich, Stirring peptide synthesis to a new level of efficiency, Org. Process Res. Dev. 26 (2022) 129–136, https://doi.org/10.1021/acs.oprd.1c00304.
[12] C. Overby, B. Abraham, E. Adjei-Sowah, A. March, K. Ling, S. Basu, D.S.W. Benoit, A rapid manual solid phase peptide synthesis method for high-throughput peptide production, J. Biomed. Mat. Res. Part A 113 (2025) e37922, https://doi.org/10.1002/jbm.a.37922.
[13] S. Duengo, M. Imam Muhajir, A.T. Hidayat, W.J.A. Musa, R. Maharani, Epimerisation in peptide synthesis, Molecules 28 (2023) 8017, https://doi.org/10.3390/molecules28248017.
[14] C. Liang, M.A.M. Behnam, T.R. Sundermann, C.D. Klein, Phenylglycine racemization in Fmoc-based solid-phase peptide synthesis: Stereochemical stability is achieved by choice of reaction conditions, Tetrahedron Lett. 58 (2017) 2325–2329, https://doi.org/10.1016/j.tetlet.2017.04.047.
[15] S. Rao Manne, A. Sharma, A. Sazonovas, A. El-Faham, B.G. de la Torre, F. Albericio, Understanding Oxyma pure as a peptide coupling additive: a guide to new Oxyma derivatives, ACS Omega 7 (2022) 6007–6023, https://doi.org/10.1021/acsomega.1c06342.
[16] Y.E. Jad, S.N. Khattab, B.G. de la Torre, T. Govender, H.G. Kruger, A. El-Faham, F. Albericio, Oxyma-B, an excellent racemization suppressor for peptide synthesis, Org. Biomol. Chem. 12 (2014) 8379–8385, https://doi.org/10.1039/c4ob01612b.
[17] R. Subirós-Funosas, A. El-Faham, F. Albericio, Low-epimerization peptide bond formation with Oxyma pure: preparation of Z-*L*-Phg-Val-OMe, Organic Synth. 90 (2013) 306–315, https://doi.org/10.1002/0471264229.os090.29.
[18] Y. Yeboue, M. Jean, G. Subra, J. Martínez, F. Lamaty, T.-X. Métro, Epimerization-free C-term activation of peptide fragments by ball milling, Org. Lett. 23 (2021) 631–635, https://doi.org/10.1021/acs.orglett.0c03209.
[19] T.K. Oost, C. Sun, R.C. Armstrong, A. Al-Assaad, S.F. Betz, T.L. Deckweth, H. Ding, S.W. Elmore, R.P. Meadows, E.T. Olejniczak, A. Oleksijew, T. Oltersdorf, S. H. Rosenberg, A.R. Shoemaker, K.J. Tomaselli, H. Zou, S.W. Fesik, Discovery of potent antagonists of the antiapoptotic protein XIAP for the treatment of cancer, J. Med. Chem. 47 (2004) 4417–4426, https://doi.org/10.1021/jm040037k.
[20] Y. Yang, Peptide racemisation, in: Side Reactions in Peptide Synthesis, Academic Press, Cambridge, MA, USA, 2016, pp. 257–292.
[21] J. Naoum, I. Alshanski, A. Gitlin-Domagalska, M. Bentolila, C. Gilon, M. Hurevich, Diffusion-enhanced amide bond formation on a solid support, Org. Proc. Res. Dev. 23 (2019) 2733–2739, https://doi.org/10.1021/acs.oprd.9b00398.
[22] A. Celi, S. Cianchetti, G. Dell'Omo, R. Pedrinelli, Angiotensin II, tissue factor and the thrombotic paradox of hypertension, Exp. Rev. Cardiov. Ther. 8 (2014) 1723–1729, https://doi.org/10.1586/erc.10.161.
[23] S.J. Paravizzini, L.M. Haugaard-Kedström, C.A. Hutton, J.A. Karas, Backbone protecting groups for enhanced peptide and protein synthesis, Angew. Chem. Int. Ed. 64 (2025) e202509939, https://doi.org/10.1002/anie.202509939.
[24] L.C. Packman, N-2-hydroxy-4-methoxybenzyl (Hmb) backbone protection strategy prevents double aspartimide formation in a 'difficult' peptide sequence, Tetrahedron Lett. 36 (1995) 7523–7526, https://doi.org/10.1016/0040-4039(95)01522-1.
[25] a) M. Mergler, F. Dick, B. Sax, P. Weiler, T. Vorherr, The aspartimide problem in Fmoc-based SPPS. Part I, J. Pept. Sci. 9 (2003) 36–46, https://doi.org/10.1002/psc.430;
b) M. Mergler, F. Dick, B. Sax, C. Stähelin, T. Vorherr, The aspartimide problem in Fmoc-based SPPS. Part II, *J. Pept. Sci.* 9 (2003) 518–526, https://doi.org/10.1002/psc.473;
c) M. Mergler, F. Dick, The aspartimide problem in Fmoc-based SPPS. Part III, J Pept. Sci. 11 (2005) 650–657, https://doi.org/10.1002/psc.668;
d) A. Monti, A. Caporale, M. Ruvo, N. Doti, Side Reaction Analysis in Solid-Phase Peptide Synthesis: A Case Study in the Glu–Asp–Tyr Motif, J. Pept. Sci. 32 (2026) e70064, https://doi.org/10.1002/psc.70064.
[26] a) O. Al Musaimi, J. Tomkins, S.M. Barry, A. Basso, X. Kou, C. Zhang, S. Serban, RSC Adv. *14* (2024) 40255;
b) L.A. Carpino, E. Krause, C. Dan Sferdean, M. Schümann, H. Fabian, M. Bienert, M. Beyermann, Synthesis of 'difficult' peptide sequences: application of a depsipeptide technique to the Jung–Redemann 10- and 26-mers and the amyloid peptide Aβ(1–42), Tetrahedron Lett. 45 (2004) 7519–7523, https://doi.org/10.1016/j.tetlet.2004.07.162.
[27] J.M. Collins, S.K. Singh, T.A. White, D.J. Cesta, C.L. Simpson, L.J. Tubb, C. L. Houser, Total wash elimination for solid phase peptide synthesis, Nat. Commun. 14 (2023) 8168, https://doi.org/10.1038/s41467-023-44074-5.
[28] M. Chinellato, S. Perin, A. Carli, L. Lastella, B. Biondi, G. Borsato, E. Di Giorgio, C. Brancolini, L. Cendron, A. Angelini, Folding of class IIa HDAC-derived peptides into α-helices upon binding to myocyte enhancer Factor-2 in complex with DNA, J. Mol. Biol. 436 (2024) 168541, https://doi.org/10.1016/j.jmb.2024.168541.
[29] Z. Romanyuk, G. Bettin, P. Brear, S. Linciano, Y. Mazzocato, S. Bonadies, I. Zanotto, C. Mazzucco, A. Monferone, M.A. Soler, G. Pasut, S. De Martin, A. Scarso, C. Heinis, S. Rothenberger, M. Hyvönen, A. Angelini, Yeast display technology enables rapid discovery of low-nanomolar macrocyclic peptide inhibitors of human angiotensin-converting enzyme 2, J. Med. Chem. 69 (7) (2026) 7689–7708, https://doi.org/10.1021/acs.jmedchem.5c02876.
[30] T. Tatsumi, K. Sasamoto, T. Matsumoto, R. Hirano, K. Oikawa, M. Nakano, M. Yoshida, K. Oisaki, M. Kanai, Practical N-to-C peptide synthesis with minimal protecting groups, Commun. Chem. 6 (2023) 231, https://doi.org/10.1038/s42004-023-01030-0.
[31] Y.E. Jad, A. Kumar, A. El-Faham, B.G. de la Torre, F. Albericio, Green transformation of solid-phase peptide synthesis, ACS Sust. Chem. Eng. 7 (2019) 3671–3683, https://doi.org/10.1021/acssuschemeng.8b06520.
[32] a) C. Jimenez-Gonzalez, C.S. Ponder, Q.B. Broxterman, J.B. Manley, Using the right green yardstick: why process mass intensity is used in the pharmaceutical industry to drive more sustainable processes, Org. Process Res. Dev. 15 (2011) 912–917, https://doi.org/10.1021/op200097d;
b) E.R. Monteith, P. Mampuys, L. Summerton, J.H. Clark, B.U.W. Maes, C. Robert McElroy, Why we might be misusing process mass intensity (PMI) and a methodology to apply it effectively as a discovery level metric, Green Chem. 22 (2020) 123–135, https://doi.org/10.1039/c9gc01537j.
[33] I. Kekessie, K. Wegner, I. Martinez, M.E. Kopach, T.D. White, J.K. Tom, M. N. Kenworthy, F. Gallou, J. Lopez, S.G. Koenig, P.R. Payne, S. Eissler, B. Arumugam, C. Li, S. Mukherjee, A. Isidro-Llobet, O. Ludemann-Hombourger, P. Richardson, J. Kittelmann, D. Sejer Pedersen, L.J. van den Bos, Process mass intensity (PMI): a holistic analysis of current peptide manufacturing processes informs sustainability in peptide synthesis, J. Org. Chem. 89 (2024) 4261–4282, https://doi.org/10.1021/acs.joc.3c01494.
[34] a) G. Vivenzio, M.C. Scala, G. Auriemma, C. Sardo, P. Campiglia, M. Sala, Application of a new green protocol in solid-phase peptide synthesis: identification of a new green solvent mixture compatible with TBEC/ETT, Green Chem. Lett. Rev. 17 (2024) 2404234, https://doi.org/10.1080/17518253.2024.2404234;
b) V. Martin, P.H.G. Egelund, H. Johansson, S. Thordal Le Quement, F. Wojcik, D. Sejer Pedersen, Greening the synthesis of peptide therapeutics: an industrial perspective, RSC Adv. 10 (2020) 42457–42492, https://doi.org/10.1039/D0RA07204D.
[35] F. Bordignon, A. Scarso, A. Angelini, Challenges and achievements of peptide synthesis in aqueous and micellar media, ChemBioChem 26 (2025) e202500099, https://doi.org/10.1002/cbic.202500099.
[36] L. Lastella, M. Zecca, P. Centomo, K. Jeřabek, F. Formaggio, I. Guryanov, A. Ricci, B. Biondi, Toward a green SPPS: the use of an innovative mesoporous pDVB support for environmentally friendly solvents, J. Pept. Sci. 31 (2025) e70038, https://doi.org/10.1002/psc.70038.
[37] L. Ferrazzano, D. Corbisiero, G. Martelli, A. Tolomelli, A. Viola, A. Ricci, W. Cabri, Green solvent mixtures for solid-phase peptide synthesis: a Dimethylformamide-free highly efficient synthesis of pharmaceutical-grade peptides, ACS Sust. Chem. Eng. 7 (2019) 12867–12877, https://doi.org/10.1021/acssuschemeng.9b01766.
[38] A. Phungula, A. Kumar, M. Kaushal, C. Tucker, L. Chen, B.G. de la Torre, F. Albericio, Aqueous solid-phase peptide synthesis (ASPPS) using standard Fmoc/tBu-protected amino acids, ACS Sust. Chem. Eng. 13 (2025) 19833–19848, https://doi.org/10.1021/acssuschemeng.5c09191.
[39] L. Pacini, M. Muthyala, L. Aguiar, R. Zitterbart, P. Rovero, A. M. Papini, Optimization of peptide synthesis time and sustainability using novel eco-friendly binary solvent systems with induction heating on an automated peptide synthesizer, J. Pept. Sci. 2024; *30*, e3605, dxoi:https://doi.org/10.1002/psc.3605.
[40] D.A. Wellings, J. Greenwood, I. Thomas, C. Hughes, W. Li, F. Lin, M. Akhter Hossain, A. Lanza, M. Meldal, J.D. Wadeal, Water-based coupling of amino acids for sustainable solid-phase peptide synthesis, Nat. Sustain. (2026), https://doi.org/10.1038/s41893-025-01761-z.
[41] R. Yoshino, Y. Tokairin, M. Kikuchi, H. Konno, Fmoc-OPhth, the reagent of Fmoc protection, Tetrahedron Lett. 58 (2017) 1600–1603, https://doi.org/10.1016/j.tetlet.2017.03.021.